Article:
Watson, George Daniel, Chan, Elliot, Leake, Mark Christian et al. (2022) Structural interplay between DNA-shape protein recognition and supercoiling: the case of IHF. Computational and Structural Biotechnology Journal. pp. 5264-5274. ISSN: 2001-0370

https://doi.org/10.1016/j.csbj.2022.09.020

Structural interplay between DNA-shape protein recognition and supercoiling: the case of IHF

George D. Watson[a], Elliot W. Chan[a], Mark C. Leake[a,b], Agnes Noy[a,*]

[a] *Department of Physics, Biological Physical Sciences Institute, University of York, York, YO10 5DD, UK*
[b] *Department of Biology, University of York, York, YO10 5NG, UK*

Abstract

The integration host factor (IHF) is a prominent example of indirect readout as it imposes one of the strongest bends on relaxed linear DNA. However, the relation between IHF and torsionally constrained DNA, as occurs physiologically, remains unclear. By using atomistic molecular dynamics simulations on DNA minicircles, we reveal, for the first time, the reciprocal influence between a DNA-bending protein and supercoiling. On one hand, the increased curvature of supercoiled DNA enhances wrapping around IHF making the final complex topologically dependent. On the other hand, IHF acts as a 'supercoiling relief' factor by compacting relaxed DNA loops and, when supercoiled, it pins the position of plectonemes in a unique and specific manner. In addition, IHF restrains under- or overtwisted DNA depending on whether the complex is formed in negatively or positively supercoiled DNA, becoming effectively a 'supercoiling buffer'. We finally provide evidence of DNA bridging by IHF and reveal that these bridges divide DNA into independent topological domains. We anticipate that the crosstalk detected here between the 'active' DNA and the multifaceted IHF could be common to other DNA-protein complexes relying on the deformation of DNA.

1. Introduction

The recognition of specific DNA sequences by proteins is not always driven by the complementary pattern of hydrogen bonds between bases and aminoacids (so-called base or direct readout), but also can be driven by sequence-dependent deformability or local DNA structural features (indirect or shape readout) [1]. In the second mechanism, DNA is distorted in conformations that significantly deviate from the ideal B-form double helix in order to optimize the protein–DNA interface [2, 3]. Prominent examples are nucleosomes in eukaryotes and nucleic-associated proteins (NAPs) in prokaryotes, which, by bending and wrapping DNA, induce looping and other complex long-range 3D arrangements [4, 5, 6]. These DNA-bending proteins have crucial roles in organizing and packaging genomes as well as facilitating basic DNA transactions like transcription and replication [7, 8].

IHF is a key and representative NAP in Gram-negative bacteria such as *Escherichia coli* that induces one of the sharpest known DNA bends, with a measured angle of around 160° [9]. The crystal structure reveals that IHF is formed by a core of α helices with a pair of extended β-ribbon arms whose tip each contains a conserved proline that intercalates between two base pairs [9]. These two intercalations stabilize strong bends 9 bp apart and facilitate wrapping of two DNA 'arms' around the protein body, tightened by electrostatic interactions between the phosphate backbone and cationic amino acids, resulting in a binding site with a length between 35-40 bp [9, 10] (Figure 1).

IHF binds preferentially to the DNA consensus sequence WATCARNNNNTTR (W is A or T, R is A or G, N is any nucleotide), which is located on the right side of the binding region and is small compared to the total length of the wrapped DNA [11] (Figure 1A). However, most of the strongest IHF binding sites include an A-tract to the left-hand side (upstream of the specific sequence) that increases affinity, the degree of bending and the length of the attached DNA site [12] (Figure 1A). IHF, thus, constitutes a clear example of a recognition arising through indirect readout [13, 14, 15]. The bends induced by this protein result in higher-order structures comprising nucleoprotein complexes that are essential to a large repertoire of biological functions, including gene regulation [16], the opening of the origin of replication [17], the CRISPR-Cas system [18], and the integration and excision of phage λ DNA [19].

*Corresponding author
Email address: agnes.noy@york.ac.uk (Agnes Noy)

Through previous studies combining atomistic molecular dynamics (MD) simulations and atomic force microscopy (AFM), we have shown that the IHF–DNA complex is far more dynamic than previously thought [10]. Building on previous work [20], we demonstrated the existence of multiple conformations and provided structural detail of two intermediate meta-stable binding states, which are also characteristic of nonspecific DNA recognition [10]. These include a half-wrapped state in which only the upstream A-tract binds to the protein; and an associated state consisting of only partial binding on each side (see Figure 1). The fully-wrapped state, which is the one described by crystallography, is only observed in the presence of the consensus sequence, where its binding on the right-hand side can only occur after the binding of the A-tract on its left-hand side (Figure 1) due to a protein allosteric change [10]. The indirect readout is thus facilitated via cooperativity between the two flanks, defining a mechanical switch on the DNA [10].

We furthermore observed the formation of large DNA–IHF aggregates in AFM images and the bridging of two DNA duplexes by a single IHF protein in MD simulations (see Figure 1) [10]. This condensating behavior is of particular importance to bacterial biofilms because IHF is located at crossing points in the extracellular DNA lattice [21] and is crucial to biofilm stability [22].

In parallel, *in vivo* DNA is organized into topologically constrained domains under torsional stress [23], to which DNA responds by supercoiling. This stress causes change on the total number of DNA turns (or linking number, Lk) which is partitioned into twist (Tw) and writhe (Wr) as $Lk = Tw + Wr$. Structures with non-zero writhe correspond to large-scale changes in the DNA, with the helix axis twisting and bending to cross over itself, forming typically plectonemes. In the cell, DNA is maintained negatively supercoiled, with a superhelical density $\sigma = \Delta Lk/Lk_0 \sim -0.06$ [24, 25], being Lk_0 the default linking number.

Due to inherent difficulties in obtaining high-resolution experimental structures of supercoiled DNA, computational approaches have become very useful tools [26, 27, 28], often giving excellent agreement with microscopy imaging [29, 30, 25]. In addition, computational studies have started to investigate the rich interplay between DNA topology and proteins, explaining, for instance, how the presence of proteins can shape topological domains [31, 32, 33, 5, 6]. Other studies including all-atom MD simulations on supercoiled circular DNA have found the emergence of additional secondary recognition sites between proteins and distal DNA that resulted in the formation of closed loops [34, 35]. However, to the best of our knowledge, no structural detail has been provided on the influence of torsional stress on DNA–protein interaction.

DNA supercoiling promotes the formation of its complex with IHF [36]: experiments have shown that the protein presents greater affinity for supercoiled DNA than for linear DNA [11, 37], and the disruption of the fully-wrapped state due to mutations on the lateral positions can be recovered by supercoiled DNA [38]. Of particular note is that many of the higher-order structures governed by IHF, such as integrative recombination, transcriptional regulation, and the CRISPR–Cas system, are known to be facilitated by DNA supercoiling [39, 40, 41]. Conversely, IHF has an influence on the long-range organization of DNA: the polymer is easier to circularize in the presence of the protein [37], and its knockout causes a re-organization of DNA supercoiling at the chromosome level [42].

Here, we provide atomic insight into the structural crosstalk between DNA supercoiling and protein indirect readout, using IHF as a model case of study. This protein is a remarkable example as it induces one of the sharpest bends on DNA. By simulating the dynamics of DNA minicircles bound to IHF, we identify the importance of supercoiling to the protein's binding mode when relying on indirect readout. We observe that enhancement on DNA flexibility and curvature by supercoiling leads to an increase of DNA-binding modes with a tendency to enhance wrapping around the protein. We also explore the entropic reduction of the conformational landscape of supercoiled DNA by IHF, as well as its capacity to constrain superhelical stress. We finally provide further insight into the formation of closed DNA loops bridged by IHF and demonstrate the formation of independent topological domains.

2. Materials and Methods

2.1. Construction of DNA minicircles

A linear 336 bp DNA fragment was built using the NAB module implemented in Amber16 [43] with a sequence based on the minicircle generated by intramolecular λ-integrase recombination [44, 30]. This sequence, containing a single IHF binding site, is given in Section 1 of the supplementary material. Six

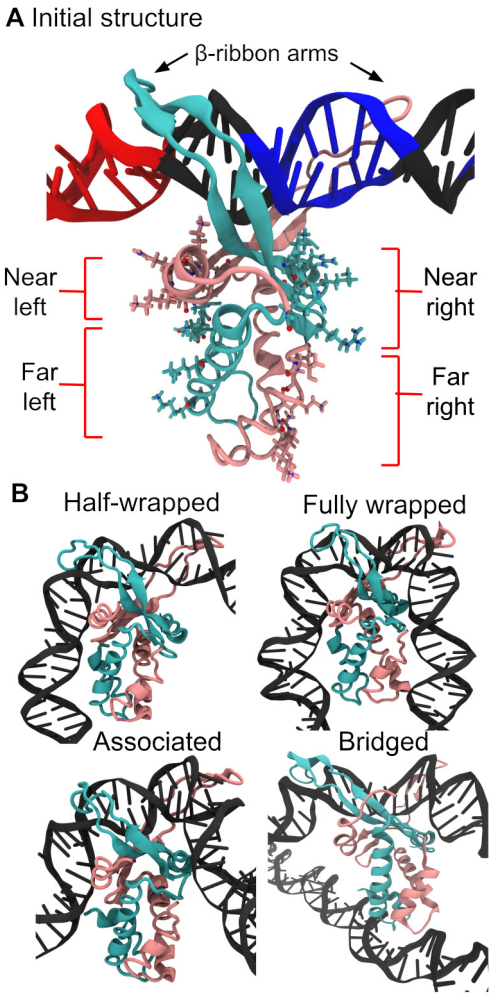

Figure 1: (A) Initial 'open' conformation for MD simulations where DNA is only bound to IHF β-ribbon arms. (B) Linear DNA then wraps around the protein presenting two meta-stable states (half-wrapped and associated state) before arriving to the fully wrapped state, if the specific sequence is present, according to a model deduced from simulations and AFM [10]. A bridged state was also observed, in which a single copy of IHF binds to two molecules of DNA [10]. The IHF α subunit is shown in mauve, β subunit in turquoise and DNA in black except when the consensus positions are highlighted in blue and the A-tract in red. The 'near' and 'far' left sites are constituted by the α and β subunits, respectively, while the 'near' and 'far' right sites are the other way round. In the half-wrapped state, the A-tract to the left binds fully while the consensus bases to the right do not interact with the protein. In the associated state, DNA binds only to the 'near' sites. In the fully wrapped state, which is the one observed by crystallography, DNA arms bind to all sites. The A-tract is always placed to the left side and the consensus positions to the right side.

perfectly planar DNA minicircles containing between 29 and 34 turns were then constructed using an in-house program as previously performed [25]. Afterwards, the structure of IHF-DNA from phage λ excision complex (Protein Data Bank (PDB): 5J0N [19]) was inserted at the matching IHF-binding H2 site contained at the attR region of the minicircle. Only the central 11-bp from H2 site that enclose the two intercalation sites was replaced by the crystallographic structure and then junctions between DNA fragments were minimized until a canonical structure was achieved, following previous studies [35]. Hence, the resultant structure used to start simulations consisted of DNA minicircles bound to IHF in an 'open state' without lateral interactions (see Figure 1).

2.2. Molecular dynamics simulations

All simulations were set up with the AMBER 16 suite of programs and performed using the CUDA implementation of AMBER's pmemd program [43]. The constructs were solvated using implicit generalized Born model at a sodium chloride salt concentration of 0.2 M with GBneck2 corrections, mbondi3 Born radii set and no cut-off for a better reproduction of molecular surfaces, salt bridges and solvation forces [45, 46, 47]. Langevin dynamics was employed for temperature regulation at 300 K with a collision frequency of 0.01 ps^1 in order to reduce the effective solvent viscosity and, thus, accelerate the exploration of conformational space [48, 10]. The protein and DNA were represented by ff14SB [49] and BSC1 [50] force fields, respectively. Prolines were kept intercalated by restraining the distances between key atoms in the proline side chain and neighboring bases [10]. Following our protocols for minimization and equilibration [10], three replica simulations of 30 ns each were performed for each topoisomer with IHF bound, and three more for the same systems with the protein removed. The first 20 ns were obtained with distance restraints on the WC canonical H-bonds to avoid a premature disruption of the double helix [35], so only the last 10 ns of each simulation were considered for analysis.

2.3. Analysis of simulations

Topological DNA twist and writhe were calculated using WrLINE, which outputs global twist and writhe values alongside the molecular contour [51]. Because global and local definitions of twist are not directly compatible [52], the accumulative twist at the DNA binding site was calculated according to the 3DNA definition at the dinucleotide level [53] using SerraNA [54]. Simulations in implicit solvent are known to systematically overestimate DNA twist [55]. To correct this, a linear fit of average writhe for bare minicircles was performed, so we could determine the value of Lk for which $Wr = 0$ (Figure S1); this was found to be $Lk_0 = 31.08$. Then, σ for each topoisomer was calculated relative to this value.

Hydrogen bonds were determined using cpptraj [56] with a distance cutoff of 3.5 Å and an angle cut-off of 120°. The number of hydrogen bonds involving each protein residue and DNA was capped at one, so time-averages along trajectories indicate the proportion of frames presenting this interaction. This was compared with the hydrogen bonds presented in the original crystallographic structure, which is the PDB entry 1IHF [9]. It should be noted that PDB 5J0N was obtained via CryoEM and posterior fitting based on 1IHF. The secondary structure of IHF was evaluated using the DSSP algorithm [57] as implemented in AMBER and grooves widths were calculated with Curves+ [58].

All simulation frames were classified via hierarchical agglomerative clustering based on the average linkage algorithm using root-mean-squared deviation (RMSd) between frames as a distance metric [56]. Only the backbone atoms of IHF and of a 61 bp region of DNA centered on the binding site were considered for the RMSd. The number of clusters was chosen so each had a distinct interaction pattern of hydrogen bonds between the protein and DNA.

3. Results and Discussion

Six different topoisomers (ΔLk=-2,-1,0,1,2,3) of DNA minircircles containing 336 bp were constructed in order to achieve a similar σ range to the one observed *in vivo* (from -0.067 to +0.094). Then, these were attached to IHF via only its protruding β-ribbon arms to simulate how DNA spontaneously wraps around the protein following an initial bound state, which resembles an encounter complex formed at the beginning of the recognition process (Figure 1) [59, 15, 10].

Three independent MD simulation replicas were performed for each topoisomer with/without IHF in implicit solvent to allow enough conformational sampling over feasible timescales (see Supplementary Movies 1-12). A continuum representation of the solvent reduces the computational cost of simulations compared with a solvation box with discrete water molecules and ions, and accelerates global structural rearrangements by at least an order of magnitude due to the neglect of solvent viscosity [30]. Although hydration and ion effects are not so accurately described, our implicitly solvated simulations reproduce well the crystallographic

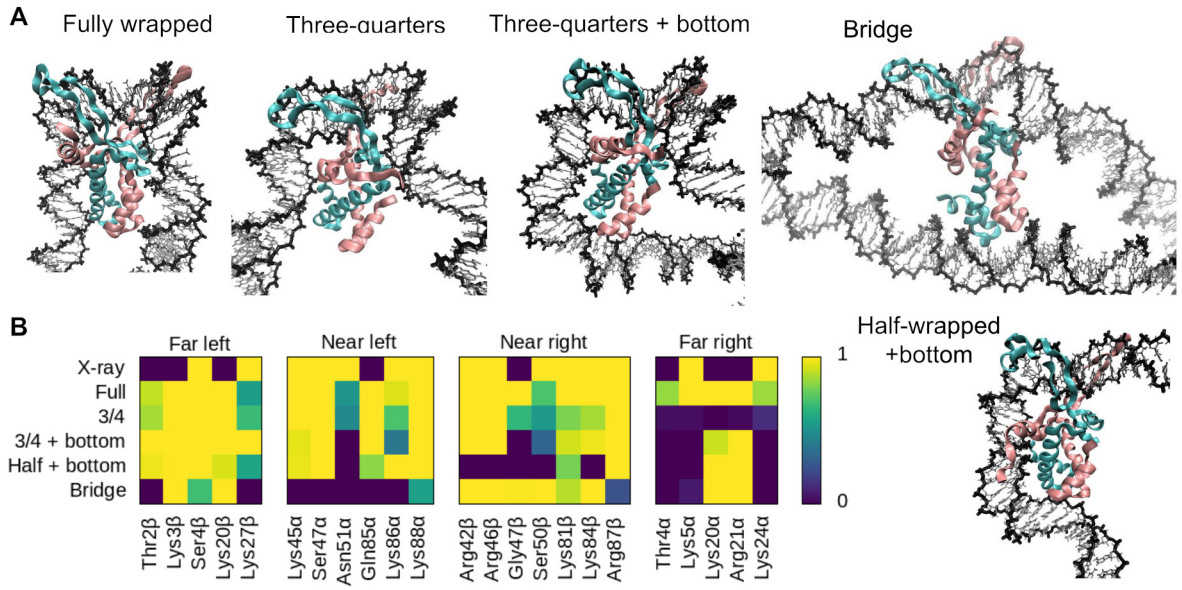

Figure 2: (A) Representative structures of the different binding modes observed in our simulations where α subunit of IHF is shown in mauve, β subunit in turquoise, A-tract is always placed to the left and the consensus positions to the right. (B) Time-average number of intermolecular hydrogen bonds formed by the main DNA-interacting amino acids belonging to each binding mode, with the crystal structure (PDB 1IHF; labeled X-ray) provided for comparison; note that the DNA in this structure is too short (35 bp) to capture some interactions in the 'far' regions.

IHF-DNA interactions (Figure 2), the protein secondary structure (Figure S2) and bp step parameters at the binding site (Figure S3). In our previous study, we also observed that this type of simulations were able to correctly capture the different IHF-DNA binding modes observed by AFM and explicitly solvated simulations in linear DNA (Figure 1) [10]. Here, we want to explore how these different complex states are influenced by the supercoiling of DNA.

3.1. DNA conformation has an active role in indirect-readout recognition

To identify the principal DNA-binding modes, all frames from all trajectories were merged together and classified into five distinct binding modes (Figure 2A) presenting a characteristic DNA-protein interaction pattern (Figure 2B) (see Methods).

As has been described previously [10], interactions between IHF and the lateral DNA arms can be divided into four regions based on their position relative to the center of the binding site and the protein subunit to which the involved amino acid belongs. On the left-hand side (containing the A-tract), the α subunit is closer to the center and thus constitutes the 'near left' site, while the β subunit is farther and composes the 'far left'. On the right-hand side (containing the consensus sequence), the α and β subunits are inversely arranged, delimiting the 'far right' and 'near right' sites, respectively (see Figure 1A).

As expected, the fully wrapped state is observed, presenting very similar protein-DNA contacts to the crystal structure [9] (Figure 2). The half-wrapped and associated states previously observed for linear DNA (Figure 1) do not appear, probably due to the inherent curvature of circular DNA (around $64°$ over a region the length of the IHF-interacting site), which can be expected to bias the system towards more tightly wrapped states. Instead, a 'three-quarters' state emerges in which the A-tract on the left binds fully to the protein while the right DNA arm binds only to the near right site. Two extra new states appear, both involving the binding of the left DNA arm to the "bottom" of the protein, while the right arm remains either unbound ('half-wrapped + bottom') or bound to only the near site ('three-quarters + bottom') (see Figure 2). Lysine 20 and Arginine 21 from the subunit α at the far right site are the aminoacids mainly responsible to wrap the left DNA arm around the "bottom" of the protein (Figure 2). We also observed a state comprising an IHF-mediated DNA bridge similar to those previously demonstrated [10], where the DNA remains relatively unbent and the two far sites or the "bottom" of the protein interact with a second DNA double helix (Figure 2).

We barely observe transitions between states over time within individual replica simulations (see Supplementary Movies 1-12). As Table 1 shows, only one simulation is observed to sample several conformations:

replica 1 for the most relaxed topoisomer switches from the three-quarters to the fully wrapped state (Supplementary Movie 5). This suggests that all of these observed binding modes are stable states corresponding to free-energy minima, where the simulations are trapped, rather than temporary transition structures en route to a global minimum, in agreement of what we found in linear DNA [10].

Our simulations reveal that the intrinsic structure and dynamics of DNA have an important role in the interaction with IHF [14], determining the extent of protein-DNA interactions and, as such, the final configuration of the complex. Hence, our study is a direct observation that DNA is not just a passive polymer to be manipulated, but it has an active role in driving the IHF recognition process [36]. Nonetheless, we still observe the same asymmetric cooperativity between sides as in linear DNA [10] (where the A-tract on the left binds first around the protein than the specific sequence on the right) because this allosteric switch depends on the protein and not on the DNA [10].

Proportion of time in the different IHF-DNA binding modes (%)

Δ Lk	σ	Full	3/4	3/4+B	Half+B	Bridge
-2	-0.067	33^{1}	33^{2}	33^{3}		
-1	-0.035	$100^{1,2,3}$				
0	0.000	21^{1}	$45^{1,2}$		33^{3}	
+1	$+0.030$	$100^{1,2,3}$				
+2	$+0.062$	$100^{1,2,3}$				
+3	$+0.094$	$67^{1,2}$				33^{3}

Table 1: Populations of the conformational states vary with the superhelical density of DNA. Percentage of simulation frames for each state and topoisomer, where 'Full' refers to the fully wrapped state, '3/4' to the three-quarters, '3/4+B' to three-quarters + bottom, 'Half+B' to half-wrapped + bottom and 'Bridge' to IHF-mediated DNA bridge. Superscripts indicate which number of replicas (1, 2 or 3) presents that corresponding state.

3.2. Supercoiling affects DNA recognition by IHF

We find that the populations of these states vary with the superhelical density of DNA (Table 1 and Figure 3). While relaxed minicircles present the fully wrapped state, they show a preference for more open states like three-quarters and half-wrapped + bottom (Supplementary Movies 5-7). These binding modes are presented approximately in equal proportion in our simulations, which is in rough agreement with the complex variability that we found in linear DNA [10]. The propensity for the fully wrapped state is strongly enhanced for moderate levels of positive and negative supercoiling, as this binding mode is presented exclusively for topoisomers ΔLk=-1,1 and 2 (Supplementary Movies 4,8 and 9). Hence, our simulations reveal that an increase in the underlying DNA curvature induced by supercoiling significantly facilitates DNA-shape readout by IHF, promoting larger wrapping around the protein compared with relaxed DNA.

We find that readout variability increases for higher superhelical densities (Figure 3): the most negatively supercoiled topoisomer (ΔLk=-2) presents different binding modes per each replica (see Supplementary Movies 1-3); the most positively supercoiled topoisomer (ΔLk=+3) results in a compact trefoil conformation in its second replica (Supplementary Movie 11) and an IHF-mediated bridge in its third (Supplementary Movie 12). As the level of torsional stress increases, DNA tends to present a broader distribution of conformations due to the emergence of extra supercoiled bends and defects in the double helix [60, 25]. These defects are associated with a wider ensemble of possible structures, because they occur stochastically at multiple sites [61, 60] and act as flexible hinges, allowing stress release and significant structural readjustments [35]. We observe the emergence of denaturation bubbles in all replica simulations of topoisomer ΔLk=-2 (see Figure 3), which presents a superhelical density close to that steadily maintained in most live bacteria (σ=-0.067) [24, 25].

Because the extent of supercoiling widely differs between chromosomal regions [62], we anticipate that the observed variability is present *in vivo*. In fact, the dependence of DNA-IHF configuration on supercoiling seems to be exploited by several biological processes, such as replication initiation [63], phage Mu transcription [64] and Tn transposition [65], as their job for IHF is conditioned upon the levels of supercoiling. For example, IHF is transformed from activator to inhibitor of Mu operator when DNA is altered from relaxed to negatively supercoiled, respectively [64]. We argue that the modulation of IHF-DNA binding modes by supercoiling revealed in our simulations could cause a change on the protein's role through an alteration of the resultant DNA architecture.

3.3. The effect of IHF on minicircle compactness and twist-writhe partition

Our simulations show that IHF globally compacts relaxed DNA loops (see Figure 4A), in agreement with previous gel electrophoresis on minicircles, where mobility was accelerated in the presence of IHF, indicating

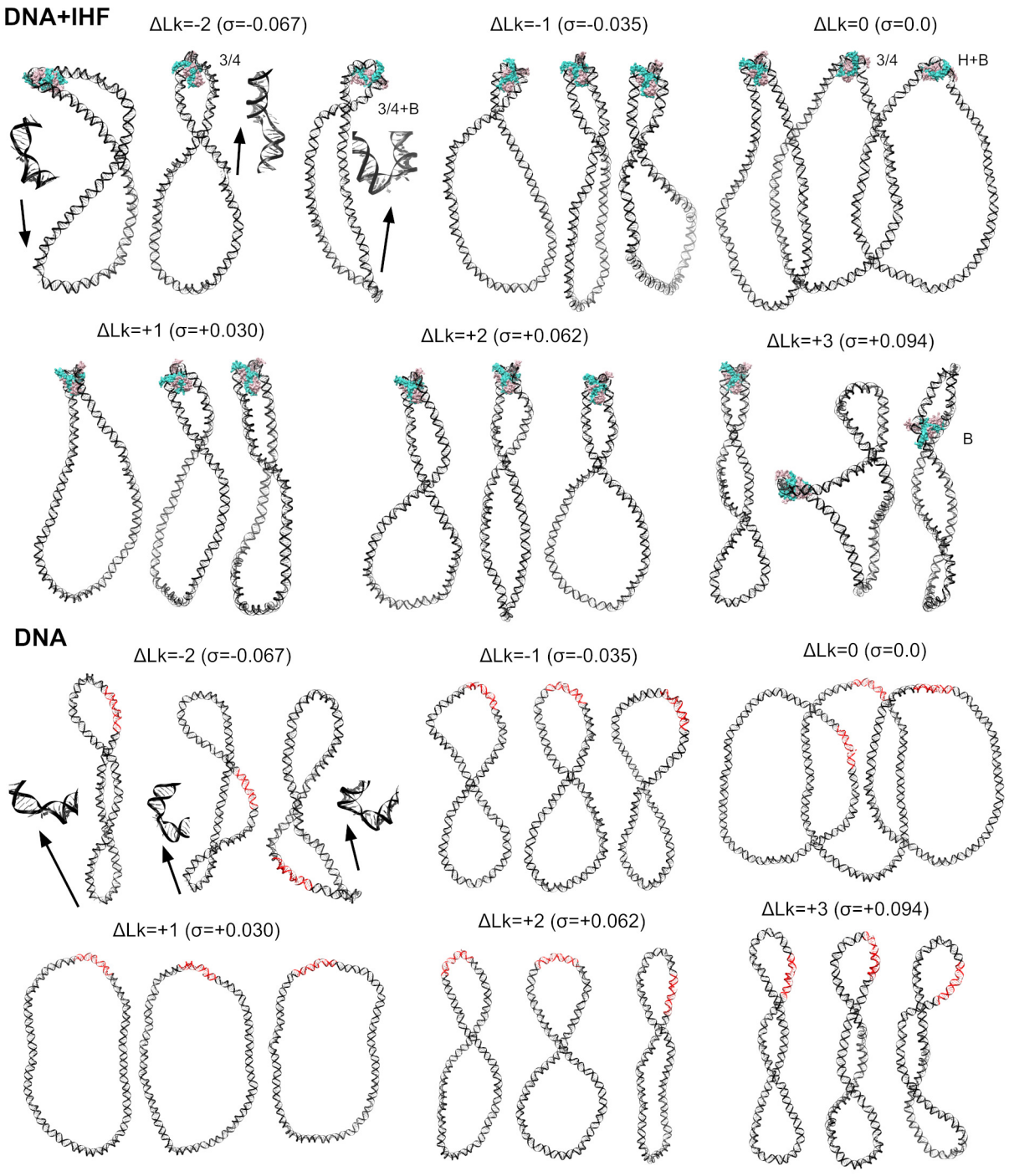

Figure 3: Overview of the dependence of the DNA-IHF interaction landscape on superhelical density given by representative structures for each individual simulation. Replicas 1, 2 and 3 for each topoisomer are displayed from left to right, respectively, and labeled with the binding mode when they not present the fully wrapped: '3/4' for the three-quarters, '3/4+B' for three-quarters + bottom, 'H+B' to half-wrapped + bottom and 'B' to IHF-mediated DNA bridge. These extra states are mainly presented on relaxed DNA (ΔLk=0) for more open conformations and on highly supercoiled DNA (ΔLk=-2,+3) promoted by enhanced flexibility and defects on the double helix (zoom-ins, indicated by arrows). IHF is mostly located at the apex of plectonemes, as opposed to bare DNA where IHF binding sites (in red) have multiple locations. Color scheme and orientation is the same as in Figure 1: α subunit of IHF is shown in mauve, β subunit in turquoise, A-tract is always placed to the left and the consensus positions to the right.

a reduction on its hydrodynamic radius [37]. We observe this effect is proportional to the level of wrapping around the protein: the first replica of topoisomer ΔLk=0, where DNA is fully wrapped, presents the strongest reduction in the radius of gyration compared with the second replica, where the DNA is wrapped three-quarter parts, and the third, where the DNA is only half wrapped (Figure 4A). As the degree of supercoiling increases in either direction, this compaction effect becomes superfluous, as DNA naturally becomes rod-like (see Figure 3 and 4). An exception to this is the ΔLk=+1 topoisomer, which remains predominantly open in the absence of IHF and becomes substantially compacted upon protein binding (Figure 4A).

IHF also brings a significant change in the twist-writhe partition on this topoisomer, which has the effect of correcting the asymmetry between positively and negatively supercoiled DNA (see Figure 4B and C). On naked DNA, negative supercoiling is associated with more writhed structures than equivalent amounts of positive supercoiling (Figure 3) [30]. However, IHF appears to correct this asymmetry by shifting the writhe of ΔLk=+1 topoisomer in the positive direction. Because twist at the binding site (Figure 4D) cannot explain the altered twist-writhe balance, we hypothesize that this effect is due to IHF-mediated bends, which stimulate writhed apex-like structures (Figure 3), enabling twist relaxation. Finally, we relate twist-writhe variability observed in topoisomer ΔLk=-2 (Figure 4B and C) to the presence of DNA defects (Figure 3). Replica 2 presents a bigger denaturation bubble compared with the other two replicas (Figure 3), which causes extremely low twist values and, as a result, a considerable moderation in writhe (Figure 4).

In summary, our simulations reveal that IHF compacts DNA loops almost as much as supercoiling, being its action especially significant on relaxed and moderately overtwisted DNA (when bare DNA is mainly in an open conformation) and becoming redundant with the increase of torsional stress. Hence, our results fit with the idea of IHF being a 'supercoiling relief' factor [66], where DNA supercoiling can be functionally replaced by IHF binding. This effect has been described in phage Mu transcription [66] and Tn transposition [65]; along with supercoiling becoming a backup for IHF in recombination [39] and CRISPR-Cas processes [41].

3.4. IHF restrains under- or overtwisted DNA depending on supercoiling direction

In the presence of IHF, our simulations reveal that the binding site presents lower or higher values of twist (between 0.5 to 1 helical turn) compared to relaxed DNA, depending on whether the complex is formed under negatively or positively supercoiled DNA, respectively (Figure 4D). The more extreme values of twist on topoisomers bound to IHF versus unbound are due to the fact that DNA wraps around the protein at the beginning of our simulations when minicircles are writhing, so most of the torsional stress is still in the form of molecular twist. In this respect, our simulations illustrate the situation of DNA being actively supercoiled and simultanously recognized by proteins, which is physiologically relevant as chromosomes are constantly transcribed and manipulated *in vivo* [67].

To understand the origin of this effect, we looked into the structures in detail and we observed a considerable amount of heterogeneity as DNA is wrapped around the protein under different levels of supercoiling (Figure 5 and S4). These conformational adjustments, which mainly consist of changes in molecular twist and groove dimensions (Figure S5), induce the protein to interact with different nucleotides, pinning the double helix in distinct orientations and thus constraining supercoiled DNA (Figure 4D, 5 and S4).

We also find that, on occasions, DNA supercoiling reduces the number of contact points between a DNA arm and its IHF side from three (encompassing two major and one minor grooves) to two (a major and a minor groove) (see the two bottom structures of Figure 5). We do not observe this conformational alteration in relaxed DNA, probably due to its natural propensity to optimally wrap IHF. Hence, our simulations reveal that the DNA conformational variability induced by supercoiling not only influences the binding modes of the complex but also its fine structural details.

Previous experiments have given an unclear picture of whether IHF constrains supercoiled DNA: while *in vivo* experiments found IHF was not able to change the overall supercoiling balance in the chromosome [68, 62], *in vitro* experiments showed that IHF had indeed the capacity to constrain supercoiled DNA on smaller plasmids [37]. Our simulations provide an explanation for these apparently contradictory results: IHF can restrain twist at the binding site, although it cannot modify the global state, because it under- or overwinds DNA depending on the supercoiling direction. In fact, our results suggest that IHF could act as a kind of 'supercoiling buffer' through the release of stored torsional stress by means of DNA breathing or dissociation as the surrounding superhelical density would change.

This view is in agreement with the concept of 'topological homeostat' associated to other NAPs like Fis, which has been detected to rescue promoters from inactivation via the formation of writhed loops, when these deviate from optimal superhelical density [69]. Our simulations suggest that IHF-induced loops could also serve this purpose of protecting promoters from supercoiling variation, apart from the more established function of facilitating their basic assemblage [70]. Interestingly, this 'torsional buffer' effect has also been exposed in eukaryotes through the reorganization of nucleosome fibers as a function of DNA twist [71]. We

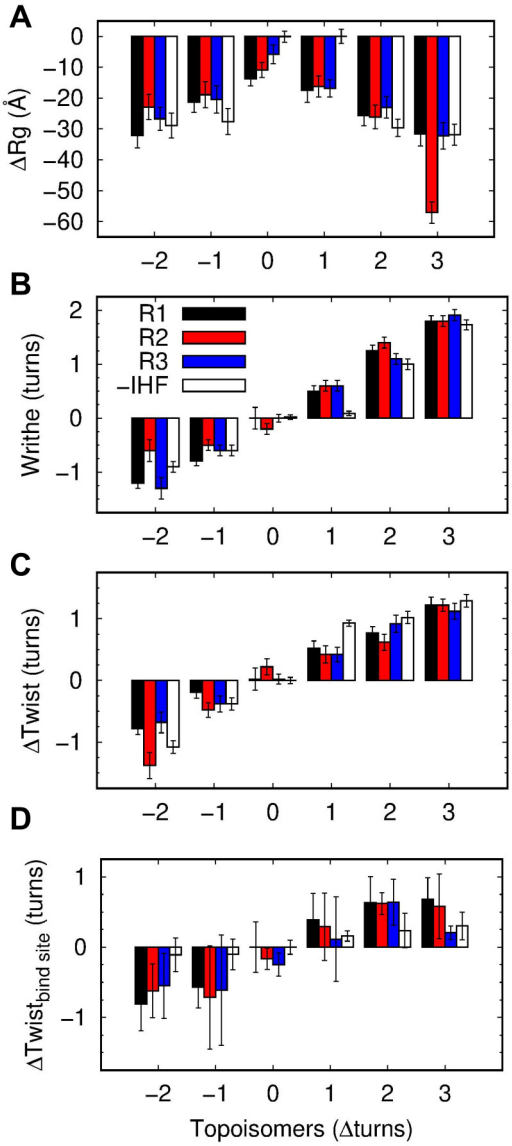

Figure 4: Averages and corresponding standard deviation (error bars) of radius of gyration (A), writhe (B), twist for the whole circle (C) and twist on the IHF binding site (D) of DNA minicircles with different levels of supercoiling, with IHF (black, red and blue for replicas 1, 2 and 3, respectively) and without IHF (white). Replica simulations are ordered from left to right as in Figure 3. The extremely low value in the radius of gyration observed for the 2nd replica of ΔLk=+3 is due to the formation of a highly compact trefoil structure (see Figure 3).

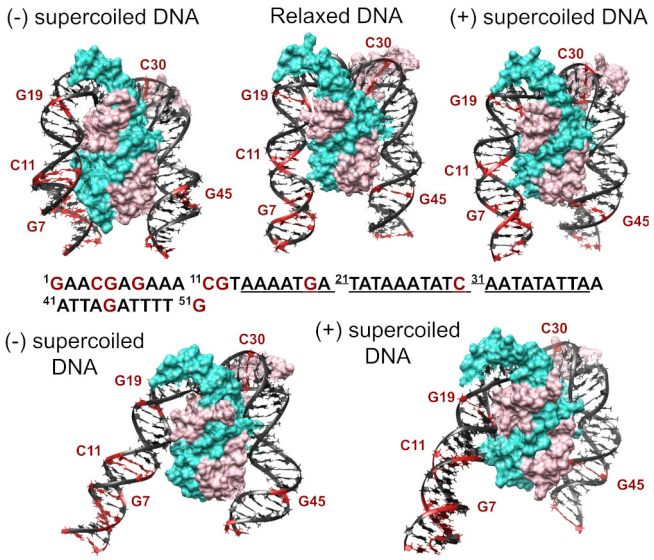

Figure 5: Supercoiling dependence of DNA structure when bound to IHF. Representative examples of the fully wrapped state formed under negatively (left) and positively (right) supercoiling reveal changes in twist compared with relaxed DNA (middle) (see Figure S5 for all replicas). The complete DNA sequence is included, where the consensus binding site is in underlined text and the most conserved positions in bold. The only few CG bp are highlighted in red and serve as rulers to compare DNA orientation relative to IHF sides. The two bottom structures reveal variability in the supercoiled DNA being fully wrapped around the protein with sizable changes in groove dimensions (right side) and a reduction in the contact points (left side). Color scheme and orientation is the same as in Figure 1: α subunit of IHF is shown in mauve, β subunit in turquoise, A-tract is always placed to the left and the consensus positions to the right.

thus point towards a general need across species of developing cushion mechanisms that can protect against supercoiling imbalance generated by crucial cellular activities, such as transcription and replication [72], as well as external factors like growth stage or environmental stress [73].

3.5. IHF reduces the entropy of the DNA supercoiling conformational landscape

In the presence of IHF, plectonemes are mostly observed to form with the protein at their apices (see Figure 3 and 6). This has the effect of significantly reducing the entropy of the minicircle conformational landscape, relative to the case in which no protein is bound (Figure 6). We observe that the conformational distribution of the DNA minicircles is significantly broader in naked DNA, as the apex of the plectoneme can be located in multiple positions. In the presence of the protein, the ensemble of conformational states is shifted towards a unique folded state, positioning the IHF at the apex.

We can quantitatively estimate the cost of the entropic reduction by using $S = k_B ln(W)$, where k_B is the Boltzmann constant and W is the number of possible states. If we assume IHF folds DNA in one state, compared with the 168 possible in naked DNA (an apex of the plectoneme can be pinned to each bp along half of the minicircle), then the entropic reduction is approximately 5.1 k_BT or 3 kcal/mol at 300 K. If we consider that not all plectoneme positions are equally probable along the naked minicircle (some conformations are more favorable than others, see Figure 3 and 6), we then need to reduce the number of states to 50 or 25%. This gives entropic penalties around 4.4 k_BT (2.6 kcal/mol) and 3.7 k_BT (2.2 kcal/mol), respectively, which are still large enough to be overcome by thermal fluctuations of bare DNA. This entropic simplification could be larger, as IHF could have the capacity to organize longer DNA loops, containing higher levels of inherent conformational variability.

Overall, our simulations support the view that IHF function consists basically of organizing DNA into unique conformations in order to facilitate the types of genetic transactions in which the protein is involved. Interestingly, a similar plectoneme-pinning effect has also been detected in damaged DNA [74, 75], showing that local changes in DNA curvature and flexibility are key to regulating the folding of supercoiled loops. This together with the fact that IHF can be functionally replaced by other DNA-bending proteins [70] suggest that the positioning of plectonemes might be a general principle for this type of architectural proteins. However, it remains an open question for future studies whether other proteins might reduce DNA conformational variability to the same degree as hardly any induces such as strong bend on DNA.

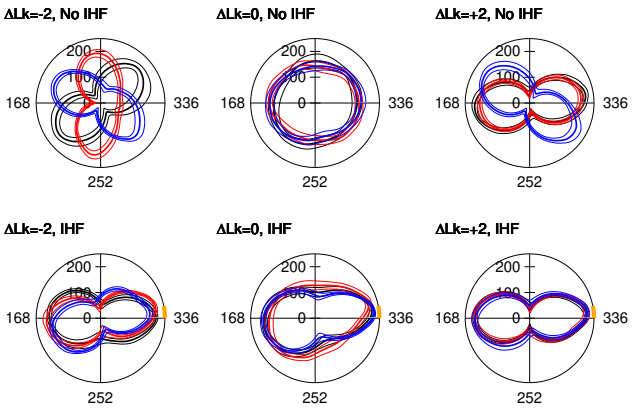

Figure 6: Polar plots of mean (± standard deviation) distance from each point along the helix axis to the DNA centroid. Each color represents a replica simulation. In the absence of IHF (top), plectonemes can form in many positions. Adding IHF (bottom, binding site location shown in orange) causes the plectonemes to align with the protein at the apex and consistently localize to the crossing points.

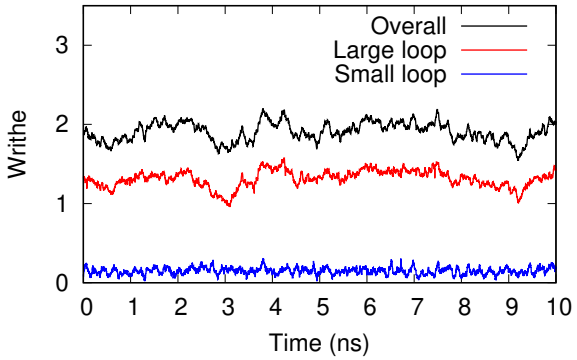

Figure 7: A DNA minicircle bridged by IHF consists of two closed loops, each of which has independent writhe. There is no evidence of writhe passing between them: the writhe of the smaller loop (81 bp, blue) remains constant, while any changes in the writhe of the larger loop (255 bp, red) are also reflected in the minicircle's overall writhe (336 bp, black).

3.6. IHF-mediated bridging divides DNA into topological domains

A DNA–IHF–DNA bridge involving additional contacts between distal DNA and the "bottom" of the protein was observed to form spontaneously in replica 3 of the most positively supercoiled minicircle ($\Delta Lk = +3$) (see Supplementary Movie 12). This bridge results from nonspecific interactions between basic aminoacids and the negatively charged DNA backbone (see Figure 2 and 3). This supports our previous findings indicating that such bridges are both possible and energetically favorable, and that specific recognition can be simply modulated or extended via additional electrostatic-driven interactions between the protein and the DNA [10].

The observation of this bridge in the most supercoiled minicircle suggests some relationship between bridge formation and supercoiling, which we explain as the result of the proximity of distal DNA sites that are far apart in torsionally relaxed DNA [40, 76, 77]. In this regard, DNA bridges involving secondary nonspecific recognition sites have also been identified for other bacterial proteins like Topoisomerase IB [34] and ParB [78] in supercoiled DNA. We think IHF needs specially high supercoiling levels to form DNA bridges ($\sigma \geq |0.095|$ or $\Delta Lk \geq |3|$, Table 1), because it naturally bends DNA. On extreme supercoiling conditions, DNA can stochastically bend and melt at a variety of points [25], giving the opportunity to avoid protein wrapping and thus to establish a bridge.

The formation of an IHF-mediated DNA bridge in a minicircle results in two closed loops. Measuring the writhe in both of these loops over time (Figure 7), reveals no evidence of writhe passing between the loops, consistent with the formation of two isolated topological domains. Furthermore, the writhe is not evenly distributed: while the larger loop accounts for 76% of the minicircle's contour length (255 bp), it holds 90% of the total writhe. That this asymmetry was not corrected by the diffusion of writhe into the smaller loop is further evidence for the separation of topological domains.

This effect can be quantified by calculating the correlation coefficients between each pair of time series: if writhe regularly passes between the two loops, one would expect the two datasets to be negatively correlated with R^2 close to 1. In fact, the calculated value is $R^2 = 0.0041$, indicating that no correlation exists between the two and that IHF is therefore demonstrably dividing the DNA minicircle into two separate topological domains. For comparison, the R^2 values for the correlation of the overall writhe with the large and small loops are 0.75 and 0.14, respectively, indicating as expected that the larger loop has a greater influence on the total writhe and that changes within both loops collectively explain almost all of the change in the minicircle's overall writhe.

Finzi and coworkers have already shown that protein-mediated DNA bridges have the capacity to establish independent topological domains, constraining variable amounts of supercoiling [79, 80]. This result was observed by specialized loop-mediating proteins like the CI [79] and *lac* repressors [80], where each DNA molecule is attached to the bridging protein by means of specific interactions. Here, our simulations provide atomic insight into this effect and reveal that a single bridge is sufficient to create a topological boundary, even if it is locked via nonspecific interactions. However, as this type of binding is weaker than specific recognition, it will probably present shorter lifetimes and, as a consequence, less capacity to define topological domains.

4. Conclusions

By performing all-atom simulations, we have provided, for the first time, atom-level insights of the interplay between DNA supercoiling and DNA-shape protein recognition (see Figure 8). We observe that changes in the intrinsic curvature of circular DNA facilitates its bending around IHF and results in the appearance of new binding modes not observed in relaxed linear DNA [10]. We also show that these effects are further enhanced by supercoiled DNA. We anticipate that the 'active role' of DNA [36] detected here for driving protein interaction (Figure 8A) will be applicable to other systems relying on indirect recognition, where DNA is heavily deformed, including other NAPs and eukaryotic chromatin-binding proteins.

As well as quantifying the influence of supercoiling on IHF binding, we also demonstrate the effect of IHF binding on the topological organization of DNA by showing that IHF strongly and reliably controls the position of plectonemes (Figure 8B). The protein also acts as a 'supercoiling relief' factor [66, 65] by inducing global compaction on relaxed DNA almost to the same extent as supercoiled loops. We anticipate that this capacity of compacting DNA and pinning plectonemes might be general to other DNA-bending proteins, although this effect is probably weaker, as barely any other protein produces a U-turn bend as IHF.

Due to the influence of DNA conformation on indirect recognition, IHF restrains under- or overtwisted DNA, depending on whether the complex is formed under negatively or positively supercoiled DNA. This effect suggests that the protein could act as a 'supercoiling buffer' by increasing or decreasing constrained supercoiled DNA as neighboring superhelical density is changed (Figure 8C). We hypothesize that IHF-induced loops could shield a supercoiling steady state on promoters for protecting their expression, as has been demonstrated by other NAPs like Fis [69]. Because eukaryotic chromatin fibers also present the capacity to homeostat DNA torsion [71], we propose that supercoiling buffering mechanisms might be essential across species to protect genome functionality from imbalances on superhelical stress.

Additional evidence [10] is also provided for DNA bridging by IHF via a secondary nonspecific interaction driven by positively charged aminoacids at the "bottom" of the protein (Figure 8D). This is only detected at extreme levels of supercoiling, because bending and melting occur stochastically at different points on the DNA, avoiding the folding of DNA arms around the protein and thus leaving the key aminoacids free. By combining the current results with our previous publication [10], we hypothesize IHF-mediated bridges to be feasible when DNA strands are nearby (*i.e.* in high DNA supercoiling levels, high DNA and counterion concentration); as well as in weak IHF binding sites where the open DNA state is significantly populated. Probably, this is of significance to a number of biofilms and to nucleoid compaction at the cellular stage when IHF is most abundant. We finally demonstrate that this bridging, even if it is based on nonspecific interactions, has the capacity to divide the DNA into two distinct topological domains.

In essence, the present study points to a collection of observations derived from the influence that DNA structure and dynamics exerts on protein recognition when based on indirect readout. This effect becomes more evident when DNA suffers from superhelical stress as it significantly changes DNA configuration energy landscape. Because this study examines DNA supercoiling within ranges observed *in vivo*, we expect our findings to be relevant in the living cell. The combination of these effects provides a biological mechanism to control DNA compaction, plectoneme positions, supercoiling and chromosome boundaries, making IHF a valuable tool for the regulation of genes in complex pathways as has been detected at the whole genomic level [42]. We anticipate that this multifaceted mode of action might not be exclusive of IHF, but it could constitute a common principle of architectural proteins responsible for the organization of chromosomes, either

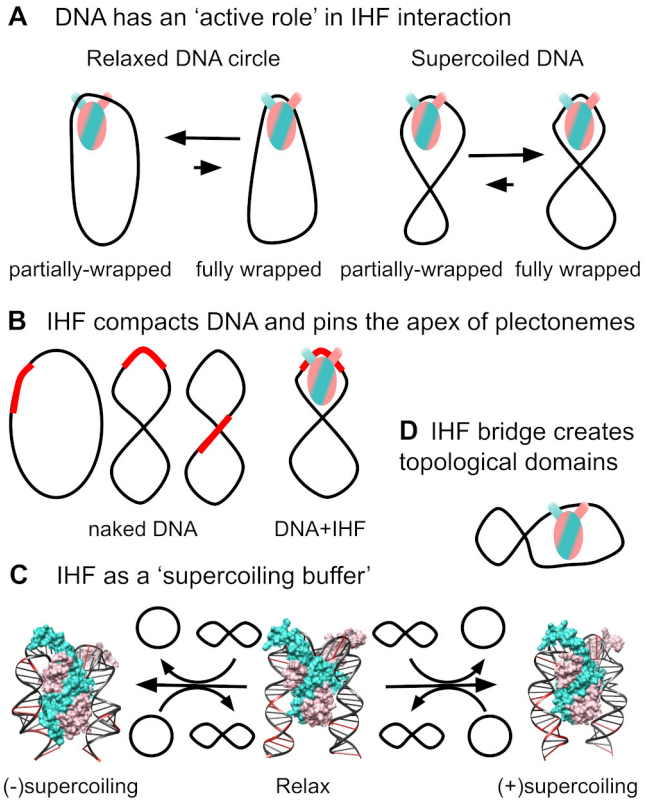

Figure 8: Model of the different ways through which the interplay between a DNA-bending protein like IHF and supercoiling emerges. (**A**) DNA intrinsic curvature facilitates wrapping around the protein, thus demonstrating DNA's active role in this recognition. (**B**) In reverse, IHF organizes DNA conformation in a unique manner through pinning curvature or plectoneme's apex. In bare DNA, the binding site (in red) can be in a variety of positions. (**C**) IHF could also act as a 'supercoiling buffer' by restraining under- or overtwisted DNA at the binding site depending on whether the complex is formed on negatively or positively supercoiled DNA, as observed in our simulations. When the neighboring supercoiling decreases or increases (represented by an open circle or an '8' shape, respectively), the constrained twisting could be released, shielding a steady supercoiling level. CG bps are in red and serve as rulers to identify differences in DNA helical pitch. (**D**) Finally, our simulations show IHF can separate DNA in topological domains through a non-specific electrostatic-driven bridging interaction. Color scheme and orientation is the same as in Figure 1: α subunit of IHF is shown in mauve, β subunit in turquoise, A-tract is always placed to the left and the consensus positions to the right.

in prokaryotes or eukaryotes, and, more generally, of proteins that recognises DNA through alterations on its shape.

Data availability

All relevant data is included in the main manuscript, the supplementary material and the University of York Data Repository (DOI 10.15124/dfc206ca-f6e1-43af-b677-8dd316d3dcf0)

Acknowledgements

Engineering and Physical Sciences Research Council (EPSRC) [EP/N027639/1, EP/T002166/1, EP/R029407/1, EP/P020259/1]; Biology and Biotechnology Research Council (BBSRC) [BB/R001235/1]; Leverhulme Trust [RPG-2017-340]; University of York Research Priming funds [ref 50109436 and G0081301]. Calculations were performed on ARCHER, JADE, Cambridge Tier-2 and the local York facilities (Viking and YARCC clusters). Funding for open access charge: York Open Access Fund. We would like to thank Daniel E. Rollins, Alice L. B. Pyne, Lynn Zechiedrich, Jonathan M. Fogg, Tom C. B. McLeish and Sarah A. Harris for useful discussions and comments.

Conflict of interest statement.

None declared.

5. CRediT authorship contribution statement

George D. Watson: Conceptualization, Validation, Formal analysis, Investigation, Data curation, Writing – original draft, Visualization. Elliot W. Chan: Validation, Fromal analysis, Writing - review editing, Visualization. Mark C. Leake: Writing – review editing, Funding acquisition. Agnes Noy: Conceptualization, Validation, Formal analysis, Writing – original draft, Writing – review editing, Visualization, Funding acquisition.

References

[1] R. Rohs, S. M. West, A. Sosinsky, P. Liu, R. S. Mann, B. Honig, The role of DNA shape in protein–DNA recognition, Nature 461 (2009) 1248–1253.

[2] J. Li, J. M. Sagendorf, T.-P. Chiu, M. Pasi, A. Perez, R. Rohs, Expanding the repertoire of DNA shape features for genome-scale studies of transcription factor binding, Nucleic Acids Res. 45 (2017) 12877–12887.

[3] F. Battistini, A. Hospital, D. Buitrago, D. Gallego, P. D. Dans, J. L. Gelpí, M. Orozco, How B-DNA dynamics decipher sequence-selective protein recognition, J. Mol. Biol. 431 (2019) 3845–3859.

[4] R. Collepardo-Guevara, T. Schlick, Chromatin fiber polymorphism triggered by variations of DNA linker lengths, Proc. Natl. Acad. Sci. U.S.A. 111 (2014) 8061–8066.

[5] S. Todolli, R. T. Young, A. S. Watkins, A. Bu Sha, J. Yager, W. K. Olson, Surprising twists in nucleosomal DNA with implication for higher-order folding, J. Mol. Biol. 433 (2021) 167121.

[6] N. Clauvelin, W. K. Olson, Synergy between protein positioning and DNA elasticity: energy minimization of protein-decorated DNA minicircles, J. Phys. Chem. B 125 (2021) 2277–2287.

[7] L. Bai, A. V. Morozov, Gene regulation by nucleosome positioning, Trends in Genetics 26 (2010) 476–483.

[8] R. T. Dame, F.-Z. M. Rashid, D. C. Grainger, Chromosome organization in bacteria: mechanistic insights into genome structure and function, Nat. Rev Genet. 21 (2020) 226–242.

[9] P. A. Rice, S. W. Yang, K. Mizuuchi, H. A. Nash, Crystal structure of an IHF-DNA complex: A protein-induced DNA U-turn, Cell 87 (1996) 1295–1306.

[10] S. Yoshua, G. Watson, J. A. L. Howard, V. Velasco-Berrelleza, M. Leake, A. Noy, Integration host factor bends and bridges DNA in a multiplicity of binding modes with varying specificity, Nucleic Acids Res. 49 (2021) 8684–8698.

[11] S. W. Yang, H. A. Nash, Comparison of protein binding to DNA in vivo and in vitro: defining an effective intracellular target., EMBO J. 14 (1995) 6292–6300.

[12] L. M. Hales, R. I. Gumport, J. F. Gardner, Examining the contribution of a dA+dT element to the conformation of Escherichia coli integration host factor-DNA complexes, Nucleic Acids Res. 24 (1996) 1780–1786.

[13] K. K. Swinger, P. A. Rice, IHF and HU: flexible architects of bent DNA, Curr. Opin. Struct. Biol. 14 (2004) 28–35.

[14] K. A. Aeling, M. L. Opel, N. R. Steffen, V. Tretyachenko-Ladokhina, G. W. Hatfield, R. H. Lathrop, D. F. Senear, Indirect recognition in sequence-specific DNA binding by Escherichia coli Integration host factor: the role of DNA deformation energy, J. Biol. Chem. 281 (51) (2006) 39236–39248.

[15] Y. Velmurugu, P. Vivas, M. Connolly, S. V. Kuznetsov, P. A. Rice, A. Ansari, Two-step interrogation then recognition of DNA binding site by Integration Host Factor: An architectural DNA-bending protein, Nucleic Acids Res. 46 (2018) 1741–1755.

[16] Y. X. Huo, Y. T. Zhang, Y. Xiao, X. Zhang, M. Buck, A. Kolb, Y. P. Wang, IHF-binding sites inhibit DNA loop formation and transcription initiation, Nucleic Acids Res. 37 (2009) 3878–3886.

[17] D. Hwang, A. Kornberg, Opening of the replication origin of Escherichia coli by DnaA protein with protein HU or IHF, J. Biol. Chem. 267 (1992) 23083–23086.

[18] A. V. Wright, J.-J. Liu, G. J. Knott, K. W. Doxzen, E. Nogales, J. A. Doudna, Structures of the CRISPR genome integration complex, Science 357 (2017) 1113–1118.

[19] G. Laxmikanthan, C. Xu, A. F. Brilot, D. Warren, L. Steele, N. Seah, W. Tong, N. Grigorieff, A. Landy, G. D. Van Duyne, Structure of a holliday junction complex reveals mechanisms governing a highly regulated DNA transaction, eLife 5 (2016) 1–23.

[20] M. Connolly, A. Arra, V. Zvoda, P. J. Steinbach, P. A. Rice, A. Ansari, Static kinks or flexible hinges: multiple conformations of bent DNA bound to integration host factor revealed by fluorescence lifetime measurements, J. Phys. Chem. B 122 (2018) 11519–11534.

[21] L. A. Novotny, A. O. Amer, M. E. Brockson, S. D. Goodman, L. O. Bakaletz, Structural stability of *Burkholderia cenocepacia* biofilms is reliant on eDNA structure and presence of a bacterial nucleic acid binding protein, PLOS ONE 8 (2013) e67629.

[22] A. Devaraj, S. S. Justice, L. O. Bakaletz, S. D. Goodman, DNABII proteins play a central role in UPEC biofilm structure, Mol. Microbiol. 96 (2015) 1119–1135.

[23] L. Postow, C. D. Hardy, J. Arsuaga, N. R. Cozzarelli, Topological domain structure of the Escherichia coli chromosome, Genes Develop. 18 (2004) 1766–1779.

[24] E. Zechiedrich, A. B. Khodursky, S. Bachellier, R. Schneider, D. Chen, D. M. Lilley, N. R. Cozzarelli, Roles of topoisomerases in maintaining steady-state DNA supercoiling in Escherichia coli, J. Biol. Chem. 275 (2000) 8103–8113.

[25] A. L. B. Pyne, A. Noy, K. H. S. Main, V. Velasco-Berrelleza, M. M. Piperakis, L. A. Mitchenall, F. M. Cugliandolo, J. G. Beton, C. E. M. Stevenson, B. W. Hoogenboom, A. D. Bates, A. Maxwell, S. A. Harris, Base-pair resolution analysis of the effect of supercoiling on DNA flexibility and major groove recognition by triplex-forming oligonucleotides, Nat. Commun. 12 (2021) 1053.

[26] F. Lankaš, R. Lavery, J. H. Maddocks, Kinking occurs during molecular dynamics simulations of small DNA minicircles, Structure 14 (2006) 1527–1534.

[27] J. S. Mitchell, C. A. Laughton, S. A. Harris, Atomistic simulations reveal bubbles, kinks and wrinkles in supercoiled DNA, Nucleic Acids Res. 39 (2011) 3928–3938.

[28] C. Matek, T. E. Ouldridge, J. P. K. Doye, A. A. Louis, Plectoneme tip bubbles: Coupled denaturation and writhing in supercoiled DNA, Sci. Rep. 5 (2015) 7655.

[29] A. Amzallag, C. Vaillant, M. Jacob, M. Unser, J. Bednar, J. D. Kahn, J. Dubochet, A. Stasiak, J. H. Maddocks, 3D reconstruction and comparison of shapes of DNA minicircles observed by cryo-electron microscopy, Nucleic Acids Res. 34 (2006) e125.

[30] R. N. Irobalieva, J. M. Fogg, D. J. Catanese, T. Sutthibutpong, M. Chen, A. K. Barker, S. J. Ludtke, S. A. Harris, M. F. Schmid, W. Chiu, L. Zechiedrich, Structural diversity of supercoiled DNA, Nat. Commun. 6 (2015) 1–10.

[31] J. Wei, L. Czapla, M. A. Grosner, D. Swigon, W. K. Olson, DNA topology confers sequence specificity to nonspecific architectural proteins, Proc. Natl. Acad. Sci. U.S.A. 111 (2014) 16742–16747.

[32] M. Pasi, R. Lavery, Structure and dynamics of DNA loops on nucleosomes studied with atomistic, microsecond-scale molecular dynamics, Nucleic Acids Res. 44 (2016) 5450–5456.

[33] M. Pasi, D. Mornico, S. Volant, A. Juchet, J. Batisse, C. Bouchier, V. Parissi, M. Ruff, R. Lavery, M. Lavigne, DNA minicircles clarify the specific role of DNA structure on retroviral integration, Nucleic Acids Res. 44 (2016) 7830–7847.

[34] I. D'Annessa, A. Coletta, T. Sutthibutpong, J. Mitchell, G. Chillemi, S. Harris, A. Desideri, Simulations of DNA topoisomerase 1B bound to supercoiled DNA reveal changes in the flexibility pattern of the enzyme and a secondary protein-DNA binding site, Nucleic Acids Res. 42 (2014) 9304–9312.

[35] A. Noy, A. Maxwell, S. A. Harris, Interference between triplex and protein binding to distal sites on supercoiled DNA, Biophys. J. 112 (2017) 523–531.

[36] J. M. Fogg, G. L. Randall, B. M. Pettitt, D. W. L. Sumners, S. A. Harris, L. Zechiedrich, Bullied no more: when and how DNA shoves proteins around, Q. Rev. Biophys. 45 (2012) 257–299.

[37] B. Teter, S. D. Goodman, D. J. Galas, DNA bending and twisting properties of integration host factor determined by DNA cyclization, Plasmid 43 (2000) 73–84.

[38] Q. Bao, H. Chen, Y. Liu, J. Yan, P. Dröge, C. A. Davey, A divalent metal-mediated switch controlling protein-induced DNA bending, J. Mol. Biol. 367 (2007) 731–740.

[39] E. Richet, P. Abcarian, H. A. Nash, The interaction of recombination proteins with supercoiled DNA: Defining the role of supercoiling in lambda integrative recombination, Cell 46 (1986) 1011–1021.

[40] D. Normanno, F. Vanzi, F. S. Pavone, Single-molecule manipulation reveals supercoiling-dependent modulation of lac repressor-mediated DNA looping , Nucleic Acids Res. 36 (2008) 2505–2513.

[41] C. J. Dorman, N. Ní Bhriain, CRISPR-Cas, DNA supercoiling, and nucleoid-associated proteins, Trends in Microbiol. 28 (2020) 19–27.

[42] S. Reverchon, S. Meyer, R. Forquet, F. Hommais, G. Muskhelishvili, W. Nasser, The nucleoid-associated protein IHF acts as a 'transcriptional domainin' protein coordinating the bacterial virulence traits with global transcription, Nucleic Acids Res. 49 (2020) 776–790.

[43] D. A. Case, et al., AMBER, v16 (2016).
URL `http://ambermd.org/`

[44] J. M. Fogg, N. Kolmakova, I. Rees, S. Magonov, H. Hansma, J. J. Perona, E. L. Zechiedrich, Exploring writhe in supercoiled minicircle DNA, J. Phys. Cond. Matt. 18 (2006) S45.

[45] H. Nguyen, D. R. Roe, C. Simmerling, Improved generalized born solvent model parameters for protein simulations, J. Chem. Theor. Comput. 9 (2013) 2020–2034.

[46] A. Perez, J. L. MacCallum, E. Brini, C. Simmerling, K. A. Dill, Grid-based backbone correction to the ff12SB protein force field for implicit-solvent simulations, J. Chem. Theor. Comput. 11 (2015) 4770–4779.

[47] H. Nguyen, A. Pérez, S. Bermeo, C. Simmerling, Refinement of generalized born implicit solvation parameters for nucleic acids and their complexes with proteins, J. Chem. Theor. Comput. 11 (2015) 3714–3728.

[48] R. Anandakrishnan, A. Drozdetski, R. C. Walker, A. V. Onufriev, Speed of conformational change: comparing explicit and implicit solvent molecular dynamics simulations., Biophys. J 108 (2015) 1153–1164.

[49] J. A. Maier, C. Martinez, K. Kasavajhala, L. Wickstrom, K. E. Hauser, C. Simmerling, ff14SB: Improving the accuracy of protein side chain and backbone parameters from ff99SB, J. Chem. Theor. Comput. 11 (2015) 3696–3713.

[50] I. Ivani, P. D. Dans, A. Noy, A. Pérez, I. Faustino, A. Hospital, J. Walther, P. Andrio, R. Goñi, A. Balaceanu, G. Portella, F. Battistini, J. L. Gelpí, C. González, M. Vendruscolo, C. A. Laughton, S. A. Harris, D. A. Case, M. Orozco, Parmbsc1: A refined force field for DNA simulations, Nat. Meth. 13 (2015) 55–58.

[51] T. Sutthibutpong, S. A. Harris, A. Noy, Comparison of molecular contours for measuring writhe in atomistic supercoiled DNA, J. Chem. Theor. Comput. 11 (2015) 2768–2775.

[52] L. A. Britton, W. K. Olson, I. Tobias, Two perspectives on the twist of DNA, J. Chem. Phys. 131 (2009) 245101.

[53] X. Lu, W. K. Olson, 3DNA: a software package for the analysis, rebuilding and visualization of three-dimensional nucleic acid structures, Nucleic Acids Res. 31 (2003) 5108–5121.

[54] V. Velasco-Berrelleza, M. Burman, J. W. Shepherd, M. C. Leake, R. Golestanian, A. Noy, SerraNA: a program to determine nucleic acids elasticity from simulation data, Phys. Chem. Chem. Phys. 22 (2020) 19254–19266.

[55] P. D. Dans, I. Faustino, F. Battistini, K. Zakrzewska, R. Lavery, M. Orozco, Unraveling the sequence-dependent polymorphic behavior of d(CpG) steps in B-DNA, Nucleic Acids Res. 42 (2014) 11304–11320.

[56] D. R. Roe, T. E. Cheatham, PTRAJ and CPPTRAJ: Software for processing and analysis of molecular dynamics trajectory data, J. Chem. Theor. Comput. 9 (2013) 3084–3095.

[57] W. Kabsch, C. Sander, Dictionary of protein secondary structure: Pattern recognition of hydrogen-bonded and geometrical features, Biopolymers 22 (12) (1983) 2577–2637.

[58] C. Blanchet, M. Pasi, K. Zakrzewska, R. Lavery, CURVES+ web server for analyzing and visualizing the helical, backbone and groove parameters of nucleic acid structures, Nucleic Acids Res. 39 (2011) 68–73.

[59] S. Sugimura, D. M. Crothers, Stepwise binding and bending of DNA by Escherichia coli integration host factor, Proc. Natl. Acad. Sci. USA 103 (2006) 18510–18514.

[60] Q. Wang, R. N. Irobalieva, W. Chiu, M. F. Schmid, J. M. Fogg, L. Zechiedrich, B. M. Pettitt, Influence of DNA sequence on the structure of minicircles under torsional stress, Nucleic Acids Res. 45 (2017) 7633–7642.

[61] T. Sutthibutpong, C. Matek, C. Benham, G. G. Slade, A. Noy, C. Laughton, J. P. Doye, A. A. Louis, S. A. Harris, Long-range correlations in the mechanics of small DNA circles under topological stress revealed by multi-scale simulation, Nucleic Acids Res. 44 (2016) 9121–9130.

[62] A. Lal, A. Dhar, A. Trostel, F. Kouzine, A. S. N. Seshasayee, S. Adhya, Genome scale patterns of supercoiling in a bacterial chromosome, Nat. Commun. 7 (2016) 11055.

[63] K. Kasho, H. Tanaka, R. Sakai, T. Katayama, Cooperative DnaA binding to the negatively supercoiled datA locus stimulates DnaA-ATP hydrolysis, J. Biol. Chem. 292 (4) (2017) 1251–1266.

[64] N. Higgins, D. Collier, M. Kilpatrick, H. Krause, Supercoiling and integration host factor change the DNA conformation and alter the flow of convergent transcription in phage Mu, J. Biol. Chem. 264 (1989) 3035–42.

[65] R. Chalmers, A. Guhathakurta, H. Benjamin, N. Kleckner, IHF modulation of Tn10 transposition: sensory transduction of supercoiling status via a proposed protein/DNA molecular spring, Cell 93 (1998) 897–908.

[66] M. Surette, B. Lavoie, G. Chaconas, Action at a distance in Mu DNA transposition: an enhancer-like element is the site of action of supercoiling relief activity by integration host factor (IHF), EMBO J. 8 (11) (1989) 3483–3489.

[67] T. B. K. Le, M. V. Imakaev, L. A. Mirny, M. T. Laub, High-resolution mapping of the spatial organization of a bacterial chromosome, Science 342 (6159) (2013) 731–734.

[68] C. D. Hardy, N. R. Cozzarelli, A genetic selection for supercoiling mutants of Escherichia coli reveals proteins implicated in chromosome structure, Mol. Microbiol. 57 (2005) 1636–1652.

[69] M. Rochman, M. Aviv, G. Glaser, G. Muskhelishvili, Promoter protection by a transcription factor acting as a local topological homeostat, EMBO reports 3 (4) (2002) 355–360.

[70] J. Pérez-Martín, V. de Lorenzo, Clues and consequences of DNA bending in transcription, Annu. Rev. Microbiol. 51 (1997) 593–628.

[71] A. Kaczmarczyk, H. Meng, O. Ordu, J. v. Noort, N. H. Dekker, Chromatin fibers stabilize nucleosomes under torsional stress, Nat. Commun. 11 (2020) 126.

[72] J. Ma, M. D. Wang, DNA supercoiling during transcription, Biophys. Rev. 8 (2016) 87.

[73] C. J. Dorman, DNA supercoiling and transcription in bacteria: a two-way street, BMC Mol. Cell Biol. 20 (2019) 26.

[74] P. R. Desai, S. Brahmachari, J. F. Marko, S. Das, K. C. Neuman, Coarse-grained modelling of DNA plectoneme pinning in the presence of base-pair mismatches, Nucleic Acids Res. 48 (2020) 10713–10725.

[75] W. Lim, F. Randisi, J. P. K. Doye, A. A. Louis, The interplay of supercoiling and thymine dimers in DNA, Nucleic Acids Res. 50 (2022) 2480–2492.

[76] K. Norregaard, M. Andersson, K. Sneppen, P. E. Nielsen, S. Brown, L. B. Oddershede, DNA supercoiling enhances cooperativity and efficiency of an epigenetic switch, Proc. Natl. Acad. Sci. U.S.A. 110 (2013) 17386–17391.

[77] Y. Yan, W. Xu, S. Kumar, A. Zhang, F. Leng, D. Dunlap, L. Finzi, Negative DNA supercoiling makes protein-mediated looping deterministic and ergodic within the bacterial doubling time, Nucleic Acids Res. 49 (2021) 11550–11559.

[78] G. L. Fisher, C. L. Pastrana, V. A. Higman, A. Koh, J. A. Taylor, A. Butterer, T. Craggs, F. Sobott, H. Murray, M. P. Crump, F. Moreno-Herrero, M. S. Dillingham, The structural basis for dynamic DNA binding and bridging interactions which condense the bacterial centromere, eLife 6 (2017) e28086.

[79] Y. Ding, C. Manzo, G. Fulcrand, F. Leng, D. Dunlap, L. Finzi, DNA supercoiling: A regulatory signal for the lambda repressor, Proc. Natl. Acad. Sci. 111 (2014) 15402–15407.

[80] Y. Yan, Y. Ding, F. Leng, D. Dunlap, L. Finzi, Protein-mediated loops in supercoiled DNA create large topological domains, Nucleic Acids Res. 46 (2018) 4417–4424.